Data Set Description: Three-Phase IGBT Two-Level Inverter for Electrical Drives

3 authors:

Marius Stender
Universität Paderborn
12 PUBLICATIONS   **75** CITATIONS

SEE PROFILE

Oliver Wallscheid
Universität Siegen
129 PUBLICATIONS   **1,682** CITATIONS

SEE PROFILE

Joachim Böcker
Universität Paderborn
309 PUBLICATIONS   **3,787** CITATIONS

SEE PROFILE

Data Set Description: Three-Phase IGBT Two-Level Inverter for Electrical Drives

Marius Stender*, Oliver Wallscheid, Joachim Böcker

Department of Power Electronics and Electrical Drives, Paderborn University, 33098 Paderborn, Germany,

*E-mail: stender@lea.upb.de

Abstract—Precise phase voltage information is mandatory in order to enable an accurate, efficient and high dynamic control performance of electric motor drives, especially if a torque-controlled operation is considered. However, most electrical drives do not measure the phase voltages online due to cost reasons, and, therefore, these have to be estimated by inverter models. Because of various nonlinear switching effects partly at nanosecond scale, an analytical white-box modeling approach is hardly feasible in a control context. Hence, data-driven inverter models seem favorable for this purpose. The acquisition procedure and the usability of the required measurement data set for the training process of such inverter models is described in this paper. Since the control utilizes pulse width modulation (PWM), the mean phase voltages for each PWM interval are the targets of the inverter model and measurements of these are stored in the data set together with other relevant signals. The data set provided comprises approximately 235 thousand samples in the complete operating range of an exemplary drive system and it is available on Kaggle [1].

Index Terms—data set, inverter, electrical drive, induction motor

I. INTRODUCTION

In a cascaded field-oriented control (FOC) for electric three-phase motors with a subordinate current control, the voltage is the control variable of the system. Deviations between the set value of the voltage and its reference are generally a disturbance and, hence, they lead to a less-than-ideal control performance of the drive. Since the voltage can be also an input variable of integrated observers, e.g. speed observers, these deviations might lead to steady-state inaccuracies or inefficiencies. This is particularly critical for induction motors because their control scheme typically includes a flux observer. To prevent these negative effects, the use of inverter models or inverter compensation schemes is highly recommended. Due to various nonlinear switching effects which arise for example from the interlocking time [2], parasitic components [3], [4], or zero current clamping (i.e. a phase current reaches zero within the interlocking time [5]), an analytical white-box modeling approach requiring simulation step times in the nanosecond range is hardly feasible in a control context. Additionally, the parametrization of these white-box models is difficult because of component deviations between the three phases [6] or insufficient information from data sheets. Thus, data-driven approaches seem to be favorable for this task [7]. To train such inverter models or compensation schemes, measurement data
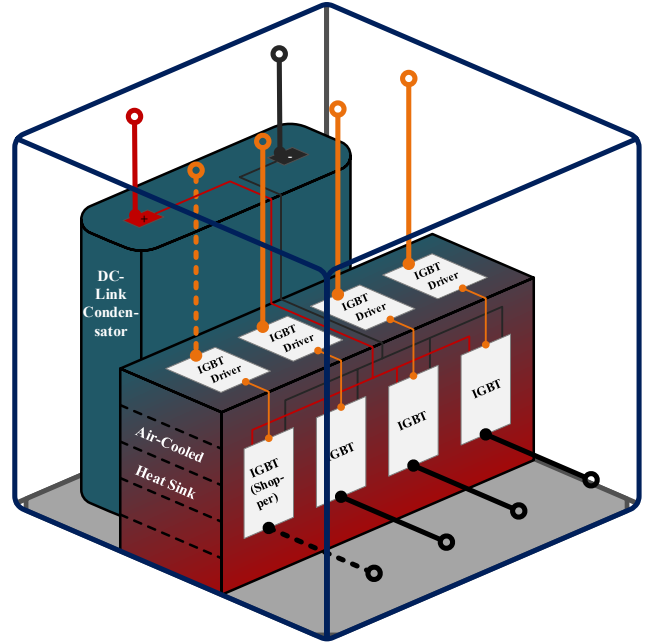
Fig. 1: Simplified structural design of the inverter with the relevant terminal connections

is required. In this paper, a published recorded data set [1] and its half-automatized acquisition process is described. At the test bench, the FOC utilizes pulse width modulation (PWM) and for each PWM interval the mean phase voltages are determined. These mean phase voltages are stored in the data set together with other relevant signals. The aim of inverter models can be stated to estimate the mean phase voltages per PWM interval as precisely as possible.

II. ACQUISITION OF THE DATA SET

A. Drive setup

In the given case, an induction motor (IM) is fed by a three-phase two-level IGBT inverter whose basic structure is visualized in Fig. 1 and its equivalent electric circuit (ECD) diagram in Fig. 2. A rapid control prototyping system (RCPS) performs the control of the motor by the use of FOC with a switching frequency of 10 kHz. The structure of the complete drive system is for a better clarity presented in Fig. 3. The rated values of the inverter and IM as well as the T-ECD

TABLE I: Characteristics of the inverter and the induction motor

Symbol	Description	Values
Inverter: SEMIKRON Semiteach IGBT		
I_{N}	Rated output current	30 A
U_{N}	Rated output voltage	400 V
U_{dc}	DC-link voltage	560 V
Induction motor: LUST ASH-22-20K13-000		
T_{N}	Nominal torque	4.7 Nm
I_{N}	Nominal phase current (star connection)	3.9 A
P_{N}	Nominal power	1.5 kW
n_{N}	Nominal speed	3000 1/min
Induction motor: identified T-ECD parameters		
R_{s}	Stator resistance	2.934 Ω
R_{r}	Rotor resistance	1.355 Ω
L_{m}	Mutual inductance	143.8 mH
L_{s}	Stator inductance	149.6 mH
L_{r}	Rotor inductance	149.6 mH
p	Number of pole pairs	2

TABLE II: Measurement and control equipment

Device	Product name
Scope	Teledyne LeCroy 12-bit HDO4104
Differential Probes	1 x PMK Bumblebee 1 kV CAT III, 2 x Teledyne LeCroy ADP305
Phase-current sensors	3 x SENSITEC CMS2015 SP10
RCPS	dSPACE MicroLabBox

motor parameters are summarized in Table I based on data sheets and basic identification processes [8].

B. Measurement structure

By means of a scope and three differential probes, the pulsating phase voltages u_{a}, u_{b}, u_{c} are measured simultaneously, comp. Fig. 4. Thereby, a 800 V voltage range and a sampling rate of $12.5 \cdot 10^6/\mathrm{s}$ are utilized at the scope which results in 2500 values per switching interval T_{s} and a quantization accuracy of approx. 0.2 V. To identify the appropriate mean phase voltages $\bar{u}_{\mathrm{a}}$, $\bar{u}_{\mathrm{b}}$, $\bar{u}_{\mathrm{c}}$ during each PWM interval, the RPCS and the scope are synchronized by a trigger signal and a signal which indicates the start of a new PWM interval. Summarizing, the voltages are recorded by the scope and all other relevant signals are recorded by the RCPS during any
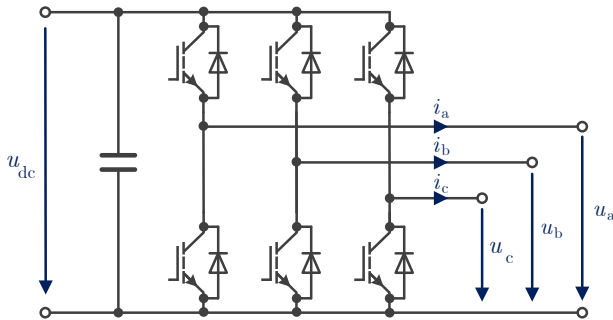

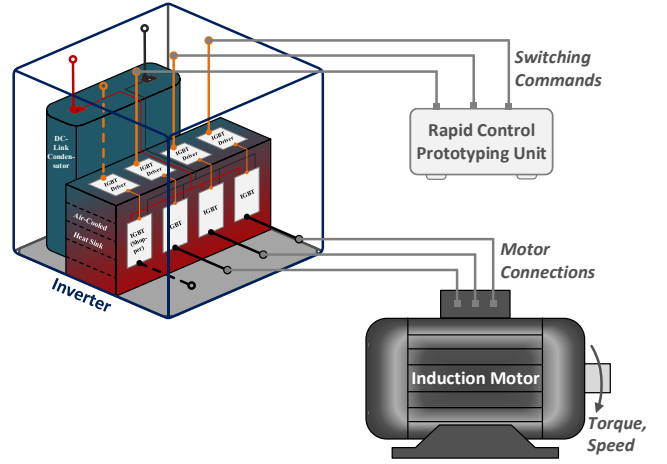Fig. 2: Equivalent circuit diagram of the inverter

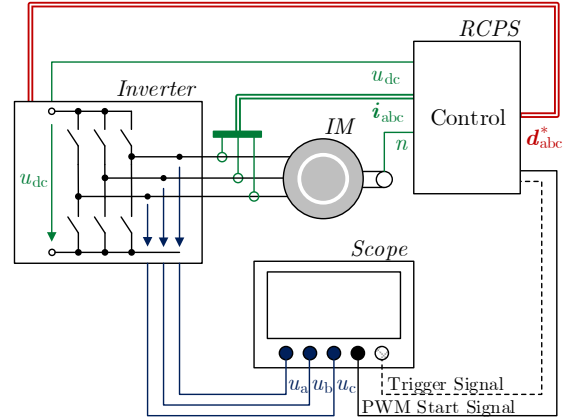Fig. 3: Integration of the inverter into the drive system

Fig. 4: Measurement structure

arbitrary operating point. The utilized specific measurement and control equipment is listed in Table II.

C. Operating mode

For being able to generate measurement data in the complete current and voltage range, the IM has to be connected to a variable mechanical load. Hereby, the IM is connected to another motor which is speed-controlled by an industrial inverter and control unit. In this configuration, at different constant speed levels the IM can be operated in current-control mode, and, thus, various duty cycle and current amplitude combinations are measurable. For some operation points, a small random signal is added to the determined duty cycle of the current controller in order to have a higher dynamic operation or reach the duty cycle limits 0 and 1 without losing the controllability of the drive.

To sum up, samples in steady-state and in dynamic operation at various motor speeds can be recorded with this configuration.

III. STRUCTURE OF THE DATA SET

The data set contains values for the phase voltages, phase currents, the duty cycles, the DC-link voltage and the speed
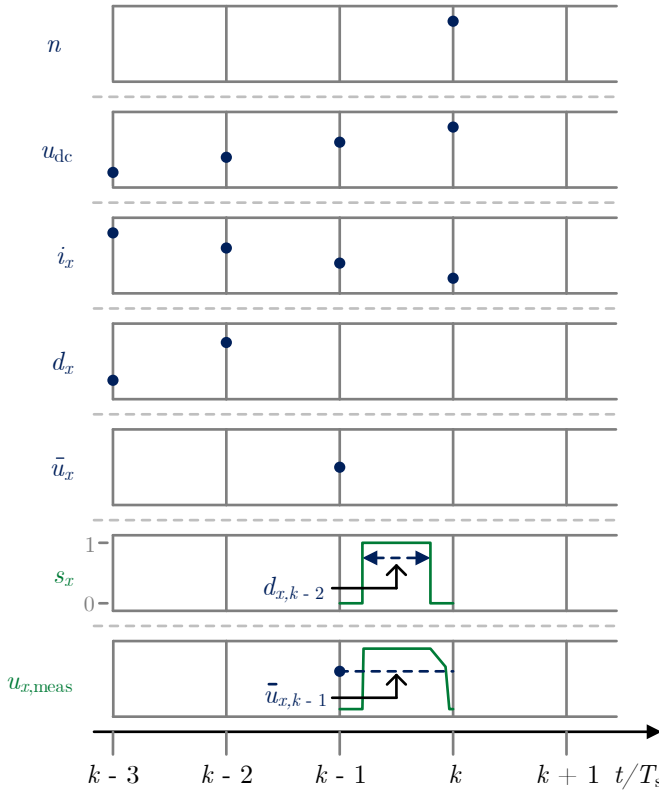
Fig. 5: Visualization of the stored signals: For each sampling step k the highlighted signal values (blue points) are stored in the data set whereas the corresponding values for all three phases $x \in [\mathrm{a,b,c}]$ are included. For clarity, the measured (green) and mean (blue) phase voltages and the switching command s_x (green) during the time interval $[k-1, k[\cdot T_\mathrm{s}$ are added into the plot. Hereby, $s_x = 1$ demands a switching action to the higher level (conducting upper transistor in phase x) and $s_x = 0$ one to the lower level (conducting lower transistor in phase x).

TABLE III: Available signals in the data set for each sampling step k

Symbol			Description	Range
n_k			Speed at k	$[404 ; 3232] /\mathrm{min}$
$u_{\mathrm{dc},k}$			DC-link voltage at k	$[548 ; 576]\,\mathrm{V}$
$u_{\mathrm{dc},k-1}$			DC-link voltage at $k-1$	$[548 ; 576]\,\mathrm{V}$
$u_{\mathrm{dc},k-2}$			DC-link voltage at $k-2$	$[548 ; 576]\,\mathrm{V}$
$u_{\mathrm{dc},k-3}$			DC-link voltage at $k-3$	$[548 ; 576]\,\mathrm{V}$
$i_{\mathrm{a},k}$	$i_{\mathrm{b},k}$	$i_{\mathrm{c},k}$	Phase currents at k	$[-7.3 ; 7.5]\,\mathrm{A}$
$i_{\mathrm{a},k-1}$	$i_{\mathrm{b},k-1}$	$i_{\mathrm{c},k-1}$	Phase currents at $k-1$	$[-7.3 ; 7.5]\,\mathrm{A}$
$i_{\mathrm{a},k-2}$	$i_{\mathrm{b},k-2}$	$i_{\mathrm{c},k-2}$	Phase currents at $k-2$	$[-7.3 ; 7.5]\,\mathrm{A}$
$i_{\mathrm{a},k-3}$	$i_{\mathrm{b},k-3}$	$i_{\mathrm{c},k-3}$	Phase currents at $k-3$	$[-7.3 ; 7.5]\,\mathrm{A}$
$d_{\mathrm{a},k-2}$	$d_{\mathrm{b},k-2}$	$d_{\mathrm{c},k-2}$	Duty cycles at $k-2$	$[0 ; 1]$
$d_{\mathrm{a},k-3}$	$d_{\mathrm{b},k-3}$	$d_{\mathrm{c},k-3}$	Duty cycles at $k-3$	$[0 ; 1]$
$\bar{u}_{\mathrm{a},k-1}$	$\bar{u}_{\mathrm{b},k-1}$	$\bar{u}_{\mathrm{c},k-1}$	Mean phase voltages at $k-1$	$[-2.3 ; 573.3]\,\mathrm{V}$
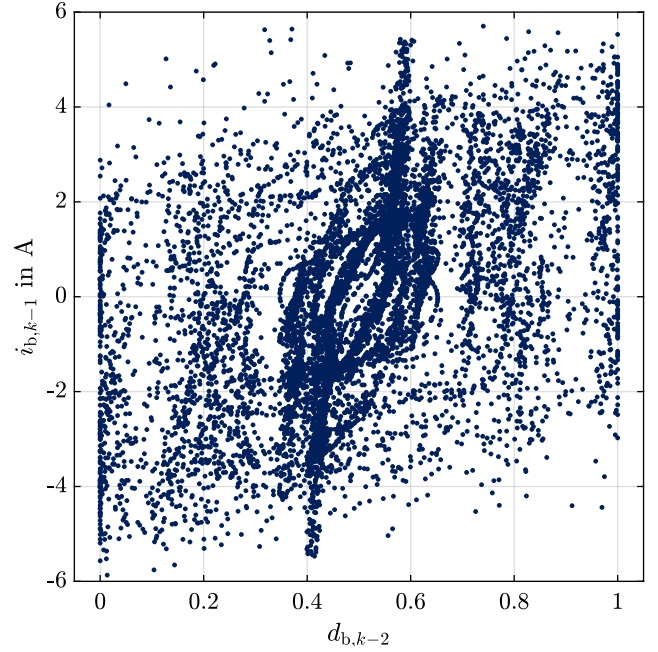
Fig. 6: Duty cycle $d_{\mathrm{b},k-2}$ and phase current value $i_{\mathrm{b},k-1}$ for randomly selected 10,000 samples of the data set

for approx. 234.5 thousand sampling steps. Since the data set is a sequence of several small recorded sequences, the signals can generally not be interpreted as continuous measurement records. Therefore, required past values of the signals for training the inverter models and inverter compensation schemes (comp. [7]) have to be included as additional signals in the data set for each sampling step. In Table III, the available signals for each sampling step are listed and in Fig. 5 their temporal link is visualized. It is to highlight, that the duty cycle $d_{x,k-2}$ of phase $x \in \{\mathrm{a,b,c}\}$ which is calculated by the RCPS during the PWM period $[k-2, k-1[\cdot T_\mathrm{s}$, is based on the measured phase currents $i_{\mathrm{a},k-2}$, $i_{\mathrm{b},k-2}$, $i_{\mathrm{c},k-2}$ and the DC-link voltage $u_{\mathrm{dc},k-2}$ during that PWM period, and is set by the inverter during the following PWM period $[k-1, k[\cdot T_\mathrm{s}$. The corresponding measured mean phase voltage is available as $u_{x,k-1}$.

For a better understanding, the set voltage of an ideal inverter (II) which does not show forward voltage drop or interlocking time effects and which has infinite sharp voltage transients and a constant DC-link voltage, can be modeled as [7]:

$$\bar{u}_{\mathrm{II},x,k-1} = d_{x,k-2} \cdot u_{\mathrm{dc},k-2} \ . \tag{1}$$

However, due to the non-ideal effects of the real inverter the measured voltage value $\bar{u}_{x,k-1}$ differs from $\bar{u}_{\mathrm{II},x,k-1}$ [7].

The data set consists of samples in the complete duty cycle and relevant current range, and exemplary, in Fig. 6 the duty cycle $d_{\mathrm{b},k-2}$ and the phase current value $i_{\mathrm{b},k-1}$ of a subset are visualized.

IV. ACCESSING THE DATA SET

The data set is published on Kaggle and can be downloaded there free of charge. The link to the data set is: https://www.kaggle.com/stender/inverter-data-set.

V. Applications of the data set

This data set can be used for training black-box inverter models and black-box inverter compensation schemes which result in high voltage accuracies, compare [7]. Thereby, the following variables of Table III can be defined as inputs and targets [7]:

Black-box inverter model:
- ○ inputs: $d_{a,k-3}, d_{b,k-3}, d_{c,k-3}, d_{a,k-2}, d_{b,k-2},$ $d_{c,k-2},\ i_{a,k-1},\ i_{b,k-1},\ i_{c,k-1},\ i_{a,k},$ $i_{b,k},\ i_{c,k},\ u_{dc,k-1},\ u_{dc,k},$
- ○ targets: $\bar{u}_{a,k-1}, \bar{u}_{b,k-1}, \bar{u}_{c,k-1},$

Black-box inverter compensation scheme:
- ○ inputs: $\bar{u}_{a,k-1},\quad \bar{u}_{b,k-1},\quad \bar{u}_{c,k-1},\quad d_{a,k-3},$ $d_{b,k-3}, d_{c,k-3}, i_{a,k-3}, i_{b,k-3}, i_{c,k-3},$ $i_{a,k-2},\quad i_{b,k-2},\quad i_{c,k-2},\quad u_{dc,k-3},$ $u_{dc,k-2},$
- ○ targets: $d_{a,k-2}, d_{b,k-2}, d_{c,k-2}$.

References

[1] M. Stender, O. Wallscheid, and J. Böcker, "Data set - three-phase igbt two-level inverter for electrical drives (data)," Jul. 2020. [Online]. Available: https://www.kaggle.com/stender/inverter-data-set

[2] Y. Murai, T. Watanabe, and H. Iwasaki, "Waveform distortion and correction circuit for pwm inverters with switching lag-times," *IEEE Transactions on Industry Applications*, vol. IA-23, no. 5, pp. 881–886, Sep. 1987.

[3] R. J. Kerkman, D. Leggate, D. W. Schlegel, and C. Winterhalter, "Effects of parasitics on the control of voltage source inverters," *IEEE Transactions on Power Electronics*, vol. 18, no. 1, pp. 140–150, Jan. 2003.

[4] Z. Zhang and L. Xu, "Dead-time compensation of inverters considering snubber and parasitic capacitance," *IEEE Transactions on Power Electronics*, vol. 29, no. 6, pp. 3179–3187, June 2014.

[5] N. Urasaki, T. Senjyu, T. Kinjo, T. Funabashi, and H. Sekine, "Dead-time compensation strategy for permanent magnet synchronous motor drive taking zero-current clamp and parasitic capacitance effects into account," *IEE Proceedings - Electric Power Applications*, vol. 152, no. 4, pp. 845–853, July 2005.

[6] S. M. Seyyedzadeh and A. Shoulaie, "Accurate modeling of the nonlinear characteristic of a voltage source inverter for better performance in near zero currents," *IEEE Transactions on Industrial Electronics*, vol. 66, no. 1, pp. 71–78, Jan 2019.

[7] M. Stender, O. Wallscheid, and J. Böcker, "Comparison of grey-box and black-box two-level IGBT three-phase inverter models for electrical drives," in *IEEE Transactions on Industrial Electronics*, 2020.

[8] IEEE, "IEEE Standard Test Procedure for Polyphase Induction Motors and Generators," *IEEE Std 112-2004 (Revision of IEEE Std 112-1996)*, pp. 1–83, 2004.